

DROSHA Knockout Leads to Enhancement of Viral Titers for Vectors Encoding miRNA-Adapted shRNAs

Hee Ho Park,^{1,2} Robinson Triboulet,^{1,4} Martin Bentler,³ Swaroopa Guda,¹ Peng Du,^{1,4} Haiming Xu,¹ Richard I. Gregory,^{1,4,5,6} Christian Brendel,^{1,5,7} and David A. Williams^{1,5,6,7}

¹Division of Hematology/Oncology, Boston Children's Hospital, Harvard Medical School, Boston, MA, USA; ²Program of Biotechnology and Bioengineering, Kangwon National University, Chuncheon, Gangwon-do 24341, Republic of Korea; ³Institute of Experimental Hematology, Hannover, Germany; ⁴Stem Cell Program, Boston Children's Hospital, Department of Biological Chemistry and Molecular Pharmacology, Harvard Medical School, Boston, MA, USA; ⁵Harvard Stem Cell Institute, Harvard University, Boston, MA, USA; ⁶Harvard Initiative for RNA Medicine, Harvard Medical School, Boston, MA, USA; ⁷Department of Pediatric Oncology, Dana-Farber Cancer Institute, Boston, MA, USA

RNAi-based gene therapy using miRNA-adapted short hairpin RNAs (shRNA^{miR}) is a powerful approach to modulate gene expression. However, we have observed low viral titers with shRNA^{miR}-containing recombinant vectors and hypothesized that this could be due to cleavage of viral genomic RNA by the endogenous microprocessor complex during virus assembly. To test this hypothesis, we targeted *DROSHA*, the core component of the microprocessor complex, and successfully generated monoallelic and biallelic *DROSHA* knockout (KO) HEK293T cells for vector production. *DROSHA* KO was verified by polymerase chain reaction (PCR) and western blot analysis. We produced lentiviral vectors containing Venus with or without shRNA hairpins and generated virus supernatants using *DROSHA* KO packaging cells. We observed an increase in the fluorescence intensity of hairpin-containing Venus transcripts in *DROSHA* KO producer cells consistent with reduced microprocessor cleavage of encoded mRNA transcripts, and recovery in the viral titer of hairpin-containing vectors compared with non-hairpin-containing constructs. We confirmed the absence of significant shRNA^{miR} processing by northern blot analysis and showed that this correlated with an increase in the amount of full-length vector genomic RNA. These findings may have important implications in future production of viral shRNA^{miR}-containing vectors for RNAi-based therapy.

INTRODUCTION

MicroRNAs (miRNAs) are a class of small regulatory RNAs of ~22 nt involved in diverse biological pathways as key post-transcriptional regulators of gene expression.¹ These miRNAs pair with complementary sites of the mRNAs and mediate post-transcriptional repression, also termed RNAi.^{2,3} RNAi-mediated gene silencing has been extensively studied in the laboratory and may provide a powerful therapeutic approach to human diseases to selectively modulate gene expression because of its high efficiency and sequence specificity.^{4,5}

Short hairpin RNAs (shRNAs) are a class of RNA polymerase (pol) III-driven shRNAs that mimic the structure of miRNA precursor intermediates.⁶ shRNAs are expressed in mammalian cells to achieve efficient knockdown; however, it has been previously reported that oversaturation of processing machinery in cells expressing shRNAs from heterologous promoters at high levels is associated with cytotoxic effects^{7–11} and increased mortality in mice in transgenic model systems.^{12,13} For clinical application of RNAi therapeutics, alternative expression systems, including both more physiologic levels of expression and the capacity to effect lineage-specific expression, may be required. This can be accomplished by embedding shRNAs into flanking miRNA scaffolds, termed miRNA-adapted shRNAs (shRNA^{miR}s), which mimic the structure of endogenous miRNAs as described previously by us and others.^{14,15}

We have recently reported a clinically applicable pol II promoter-driven viral shRNA^{miR} vector for knocking down *BCL11A* with improved efficiency and less cytotoxicity.^{14,15} *BCL11A* interacts with other transcription factors to repress the γ -globin (fetal) gene during adult life leading to increased β -globin (adult) gene expression.^{16,17} The molecular switch from fetal to adult globin is associated with emergence of signs and symptoms of sickle cell disease (SCD) and β -thalassemias in individuals with β -globin mutations.^{16,18} One therapeutic approach to treatment of β -hemoglobinopathies is the knock-down of *BCL11A*, which simultaneously restores γ -globin gene expression and reduces mutant β -globin expression (NCT03282656).

Received 2 July 2018; accepted 2 July 2018;
<https://doi.org/10.1016/j.omtn.2018.07.002>

Correspondence: David A. Williams, Division of Hematology/Oncology, Boston Children's Hospital, 300 Longwood Ave., Karp 08125.3, Boston, MA 02115, USA.
E-mail: dawilliams@childrens.harvard.edu



Endogenous miRNAs are transcribed as primary transcripts (pri-miRNA), which are cleaved by the microprocessor complex, DROSHA-DGCR8.¹⁹ DGCR8 binds to the hairpin and directs RNase III-like endonuclease DROSHA to the intended cleavage site.^{20–22} Alternatively, DROSHA itself can also bind to the pri-miRNA and perform endonucleolytic cleavage.²³ Subsequently, the pre-miRNA is exported from the nucleus to the cytoplasm by Exportin-5 and further processed by Dicer.²⁴ The resulting small interfering RNA (siRNA) duplex binds to the Argonaute (Argo-) protein subunit of the RNA-induced silencing complex (RISC), where strand selection and target mRNA cleavage occur.²⁵

We observed that the viral titers of hairpin shRNA^{miR} vectors were consistently lower than non-hairpin-containing vectors. We hypothesized that low recombinant viral titers were due to cleavage of viral genomic RNA by the endogenous microprocessor complex during virus assembly in vector packaging cells. To test this hypothesis, we generated knockout (KO) of DROSHA, the core catalytic component of the microprocessor complex, in viral vector packaging cells by deleting exons 4–30 using CRISPR/Cas9.²⁶ The *DROSHA* KO cell lines were tested for generation of hairpin shRNA^{miR} recombinant virus. We demonstrate a recovery of viral titer and show correlation of the absence of shRNA^{miR} processing, and an increase in the amount of full-length vector genomic RNA in both producer cells and viral particles. These insights are important for the clinical development of any hairpin-containing viral vectors that induce RNAi to treat diseases.

RESULTS

DROSHA KO Strategy Using CRISPR/Cas9

To determine the influence of miRNA processing on the lower titers observed in shRNA-containing vectors, we targeted the *DROSHA*-DGCR8 microprocessor complex for deletion. We utilized a CRISPR/Cas9 vector, pX458, for the co-expression of single guide RNAs (sgRNAs), SpCas9, and a GFP reporter (Figure 1A).²⁶ The *DROSHA* gene is located on chromosome 5, spans 132 kb, and consists of 35 exons with the start codon in exon 3 (Figure 1B).²³ We selected two sgRNAs targeting the 5' end of exon 4 (labeled gRNAs 1–2) of *DROSHA* and two guide RNAs (gRNAs) targeting the 3' end of exon 30 (labeled gRNAs 3–4) (Table S1) to affect a deletion of nearly the entire coding region.

We co-transfected combinations of 5' and 3' targeting gRNAs into HEK293T/17 cells and sorted GFP high-expressing cells. Sorted cells were plated at low density, and resulting colonies were picked individually to establish clonal cell lines. The clones were screened by polymerase chain reaction (PCR) analysis to identify a complete *DROSHA* (D) KO cell line using *DROSHA*-specific primers (Figure 1C, top). In parental wild-type (WT) cells, PCR bands of 331 and 345 bp in lane 1 (primers 1 and 2) and lane 2 (primers 3 and 4) were observed, representing the 5' and 3' junctions of the targeted region (Figure 1C, top panel). For heterozygous KO, additional PCR bands of 421 bp in lane 4 (primers 1 and 3) and 255 bp in lane 5 (primers 2 and 4) indicate inversion of one allele (Figure 1C, middle panel), thereby inacti-

vating this allele. For homozygous KO, PCR bands of 421 bp in lane 4 (primers 1 and 3) and 255 bp in lane 5 (primers 2 and 4) indicate inversion of both alleles and complete inactivation of the *DROSHA* gene (Figure 1C, lower panel at arrowheads). As seen in WT, heterozygous KO, and homozygous KO, the PCR product of 402 bp is absent in lane 3 (primers 1 and 3), indicating that complete deletion of the targeted fragment did not occur. We next confirmed the complete loss of DROSHA protein by immunoblot analysis (Figure 1D). For WT, the expected DROSHA protein band was observed at 170 kDa in lane 1. For homozygous deletion, the absence of DROSHA protein is confirmed in lane 3. In case of the heterozygous KO, the re-arrangement of one allele leads to an ~50% reduction in band intensity (lane 2). We next determined the effect of reduced DROSHA expression on cell growth (Figure 1E). Complete absence of DROSHA protein was associated with significantly lower proliferation compared with either WT or the single-allele rearranged clone.

Characterization of *DROSHA* KO Cell Lines

We next determined the effect of *DROSHA* KO on the capacity of cells to cleave an RNA hairpin embedded in a lentivirus vector. We constructed a control non-hairpin-containing plasmid (LeGO-SFFV) by removing the BCL11A shRNA^{miR} hairpin from the LeGO-SFFV-shRNA^{miR5} plasmid (Figure 2A).¹⁴ In LeGO-SFFV-shRNA^{miR5}, the shRNA is embedded in an miRNA223 scaffold (shRNA^{miR}) to allow expression from pol II promoters in mammalian cells. Plasmids were transfected into WT or homozygous KO cells, and northern blot was performed using a labeled RNA probe to determine the presence or absence of a processed small RNA derived from shRNA^{miR5} (Figure 2B). In WT cells transfected with the hairpin-containing plasmid (LeGO-SFFV-shRNA^{miR5}), we detected a 20-bp small RNA band representing the mature siRNA (Figure 2B, lane 3) not present in cells transfected with the construct lacking the hairpin (Figure 2B, lane 2). In contrast, we detected very little or no corresponding band in homozygous KO cells after transfection of the shRNA^{miR}-containing plasmid (Figure 2B, lane 6), indicating no or very little cleavage of the embedded shRNA in these cells. As expected, no processing of the RNA was seen when the plasmid lacking the shRNA^{miR} was transfected into homozygous KO cells (Figure 2B, lane 5). These data confirm that the absence of DROSHA severely compromises the capacity of cells to properly process and cleave shRNA^{miR} hairpin structures.

DROSHA KO in 293T Producer Cells Leads to Increased Levels of Full-Length Viral Genomic RNA for Hairpin Vectors

In order to determine the effect of miRNA processing on the generation of full-length viral genomic RNA during virus production, we performed northern blot analysis targeting the stem region of the hairpin on cell lysates of 293T packaging cell lines transfected with the plasmids shown in Figure 2A. The intensity of ribosomal 28S and 18S RNAs was used to ensure equal RNA loading in each lane of the northern blot (Figure 3A). In WT cells, we observed a relative decrease in the viral genomic length RNA transcript band intensity (at arrowhead) for the hairpin shRNA^{miR}-containing (LeGO-SFFV-shRNA^{miR5}) plasmid (Figure 3A, lane 3) compared with the

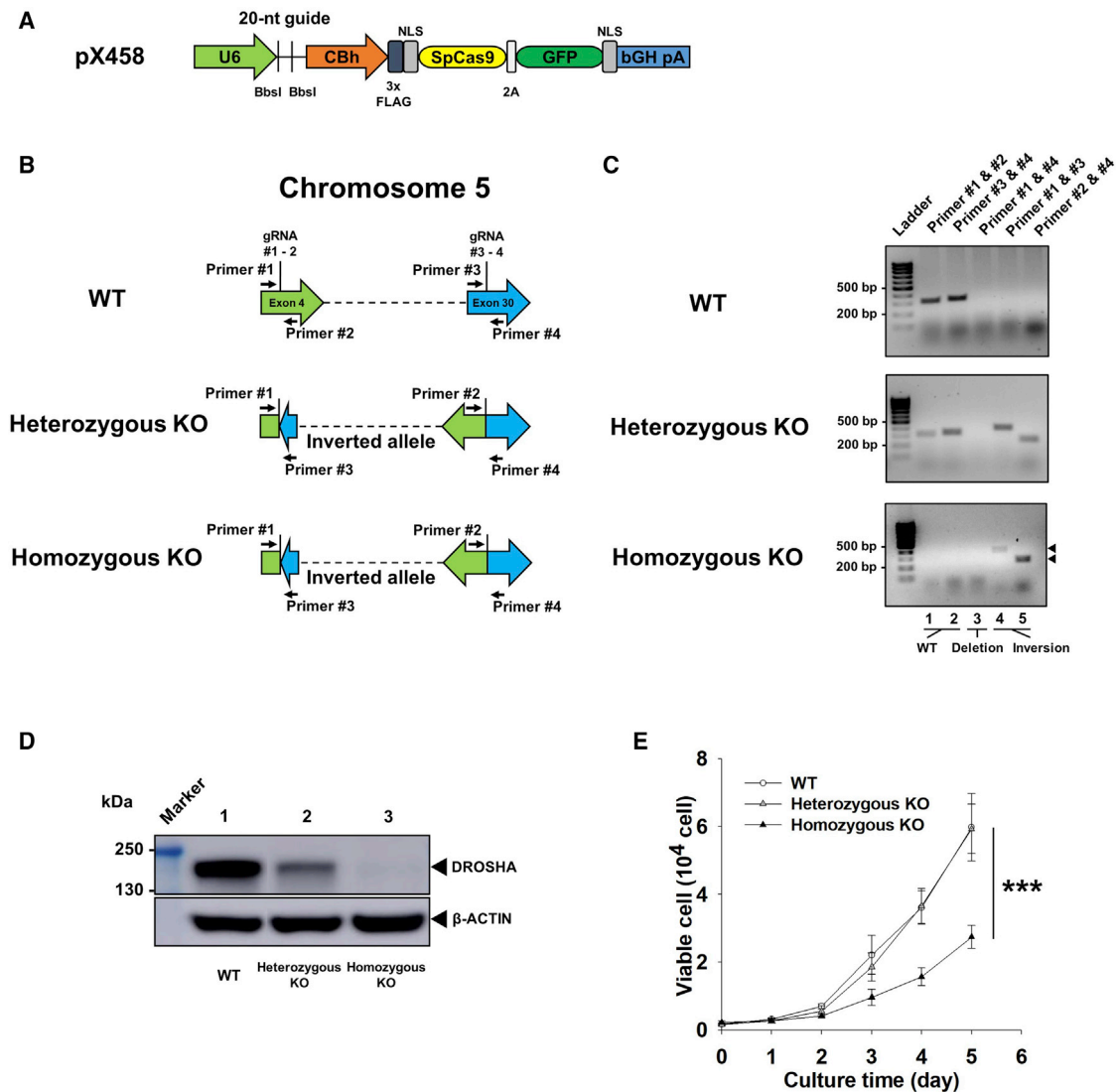


Figure 1. Strategy for Microprocessor KO in 293T Producer Cells Using CRISPR/Cas9 Gene Editing

(A) Construction of a CRISPR/Cas9 targeting vector, pX458 [labeled as pSpCas9(BB)-2A-GFP in Ran et al.²⁶]. pX458 contains the U6 promoter for the expression of guide RNA (gRNA) and the CBh promoter for ubiquitous expression of SpCas9 and GFP. Vertical lines represent insertion of 20-nt guide sequence using BbsI restriction enzyme for the expression of gRNA. (B) Strategy to target *DROSHA* on chromosome 5 using CRISPR/Cas9 and the genomic configurations of WT, heterozygous KO, and homozygous KO cell lines. For *DROSHA* KO, two gRNAs targeting the 5' end of exon 4 (labeled gRNAs 1–2 at green arrow) and two gRNAs targeting the 3' end of exon 30 (labeled gRNAs 3–4 at blue arrow) were used (solid lines and Table S1) in pairwise combinations. Black arrows represent locations of primers used for PCR analysis. (C) PCR analysis using a set of *DROSHA* primers for WT, heterozygous KO, and homozygous KO cell lines. Primers used for each lane are shown at the top. No band in lanes 1 and 2 indicates complete *DROSHA* KO (homozygous KO). No band in lane 3 indicates no deletion has taken place for allele. PCR bands in lanes 4 and 5 (arrowheads) indicate inversion of alleles. Primers are listed in Table S2. (D) Immunoblot analysis of *DROSHA* in WT, heterozygous KO, and homozygous KO cell lines. (E) Proliferation of WT (white circles), heterozygous KO (gray triangles), and homozygous KO (black triangles) 293T cell lines using CyQUANT Cell Proliferation Assay kit. Error bars: SD (N = 6). ***p < 0.0005, homozygous KO compared with the WT group. 2A, self-cleaving peptide; 3× FLAG, 3 tandem FLAG epitopes; bGH, bovine growth hormone poly A; CBh, hybrid chicken β-actin promoter; NLS, nuclear localization sequence; SpCas9, *Streptococcus pyogenes* Cas9.

non-hairpin-containing (LeGO-SFFV) plasmid (Figure 3A, lane 2). In homozygous KO cells, there was no decrease in the intensity of this full-length genomic transcript (Figure 3A, lane 6) compared with the non-hairpin-containing plasmid (Figure 3A, lane 5). In multiple independent experiments, although the total amount of

genomic mRNA varied, the ratios of genomic mRNA in WT or homozygous KO cells with or without shRNA remained consistent. Densitometric quantitation confirmed that there was an ~30% reduction of full-length genomic RNA for the hairpin-containing plasmid in WT cells and not in the homozygous KO cell line (Figure 3B).

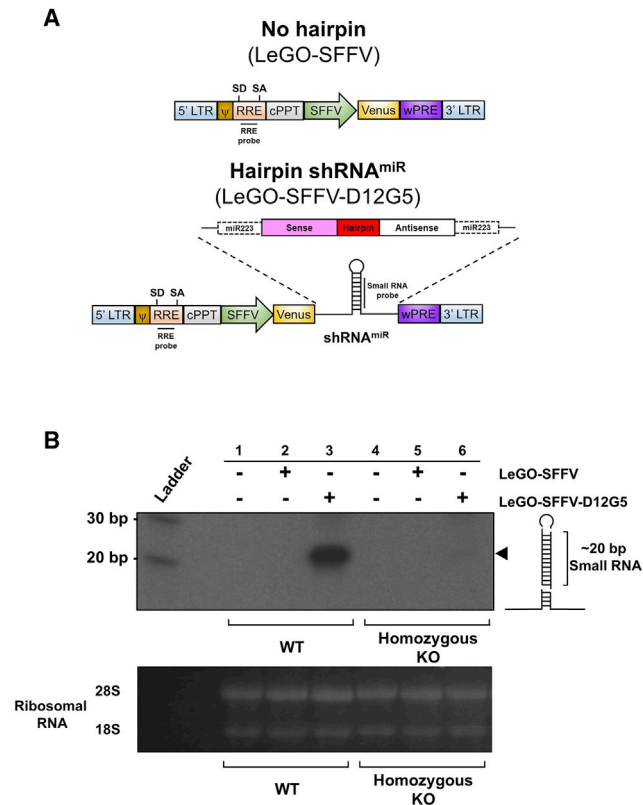


Figure 2. Characterization of Homozygous DROSHA KO Cell Line

(A) Configuration of non-hairpin-containing (LeGO-SFFV) and shRNA^{miR}-containing hairpin (LeGO-SFFV-shRNA^{miR5}) lentiviral vectors. Position of the small RNA probe or RRE probe (straight line) used for northern blot analyses is indicated. (B) Northern blot of homozygous KO cell lines to determine presence of a 20-bp siRNA product processed from the shRNA^{miR} (structure shown on right). Small RNA probe was used for the detection of cleaved stem structure of hairpin. The position of 20-bp stem structure band is noted by arrowhead. Label at top indicates homozygous KO cell lines transfected with either non-hairpin-containing (LeGO-SFFV) or hairpin shRNA^{miR}-containing (LeGO-SFFV-shRNA^{miR5}) plasmid. Ribosomal RNAs served as loading control (lower panel). ψ , packaging signal; cPPT central polypurine tract; LTR, long-terminal repeat; RRE, REV-responsive element; SA, splice acceptor; SD, splice donor; SFFV, spleen focus-forming virus promoter; wPRE, woodchuck hepatitis virus post-transcriptional regulatory element.

DROSHA KO Leads to an Increase in the Full-Length Viral Genomic RNA for Hairpin-Containing Vectors in Viral Particles

In order to determine whether the change in full-length mRNA expression was associated with an increase in full-length viral genomic RNA transcript in packaged virions, we performed northern blot analysis on virus particles generated from 293T packaging cell lines. Similar to findings in packaging cell line lysates, we observed a decrease in the viral genomic RNA transcript band intensity in virus particles harvested from WT producer cells for the hairpin shRNA^{miR}-containing (LeGO-SFFV-shRNA^{miR5}) compared with non-hairpin-containing (LeGO-SFFV) virus (Figure 4A). In contrast, we saw no apparent reduction in viral genomic RNA transcript band intensities for the hairpin shRNA^{miR}-containing (LeGO-SFFV-

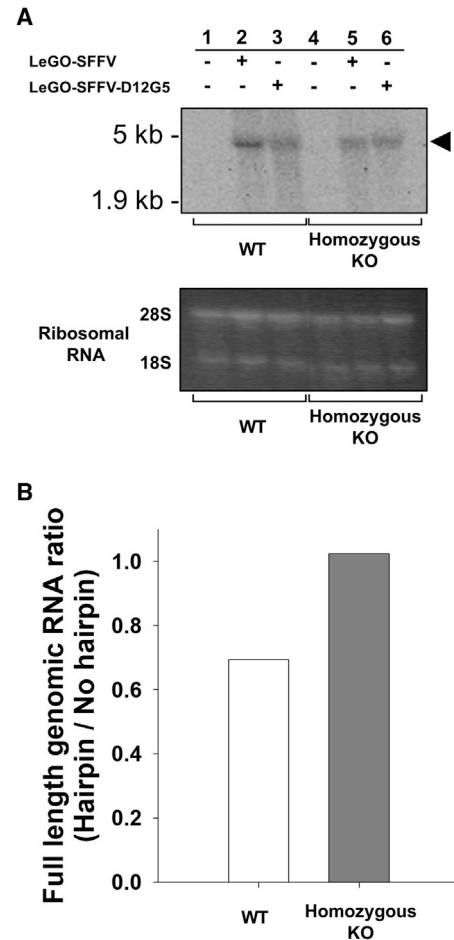


Figure 3. Cleavage of Viral Genomic RNA by Microprocessor in 293T WT Producer Cells

(A) Northern blot analysis detecting full-length viral genomic RNA in WT and homozygous Drosha KO cell lines using an RRE probe (upper panel). Label at top indicates homozygous KO cell line transfected with either non-hairpin-containing (LeGO-SFFV) or hairpin shRNA^{miR}-containing (LeGO-SFFV-shRNA^{miR5}) plasmids. Ribosomal RNAs served as loading control (lower panel). The position of the viral genomic RNA transcript band is noted by the arrowhead. (B) Densitometric quantitation of the ratio of hairpin:non-hairpin RNA bands from northern blot in (A).

shRNA^{miR5}) compared with non-hairpin-containing (LeGO-SFFV) virus. Densitometric quantitation from the northern blot analysis of the full-length genomic RNA confirmed an ~40%–50% reduction of full-length genomic RNA in viral particles containing the hairpin from WT cells with a ratio of ~0.9 in viral particles from the homozygous KO cell line (Figure 4B).

DROSHA KO Leads to an Increase in the Viral Titer for Hairpin Vectors

To determine the effect of the lack of DROSHA activity on recombinant virus production, we next compared the titer of supernatant virus production, we next compared the titer of supernatant harvested from populations of transfected 293T packaging cells on murine erythroleukemia (MEL) cells. We compared the titers

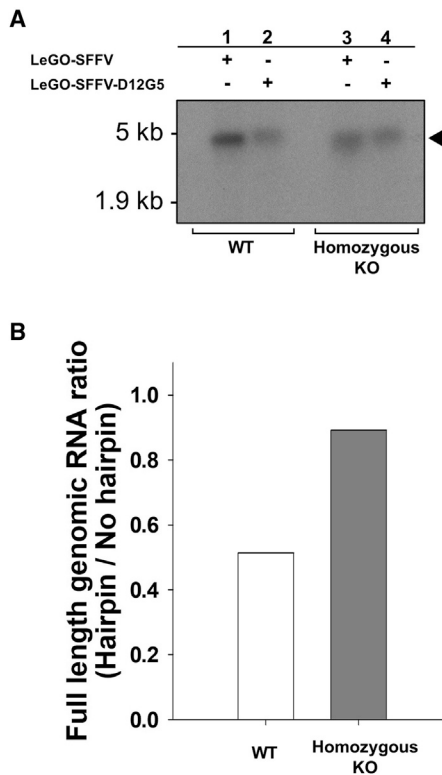


Figure 4. Detection of Full-Length Viral Genomic RNA in Viral Particles Generated from Homozygous Drosha KO Producer Cells

(A) Northern blot analysis of viral genomic RNA isolated from vector supernatants produced by transfected WT and homozygous Drosha KO cell lines using an RRE probe. Label at top indicates cell lines transfected with either non-hairpin-containing (LeGO-SFFV) or hairpin shRNA^{mir5}-containing (LeGO-SFFV-shRNA^{mir5}) plasmids. The position of viral genomic RNA transcript band is noted by an arrowhead. (B) Densitometric quantitation of the ratio of hairpin: no hairpin from northern blot in (A).

produced in heterozygous KO and homozygous KO producer cells versus WT cells as a ratio of the titer of hairpin- to no-hairpin-containing vectors (Figure 5A). In WT cells, we confirmed an ~40% decrease in the relative viral titer of hairpin compared with non-hairpin-containing vectors. In producer cells deficient in DROSHA, no decrease in the viral titer was seen, with the viral titer ratio close to 1. There appeared to be a dosage dependency on DROSHA protein expressed in the cell, because producer cells with one allele disruption and ~50% DROSHA protein showed an intermediate decrease in viral titer and viral titer ratio between 0.7 and 0.8.

Because the vector-encoded mRNA contains the Venus fluorescent reporter and the shRNA^{mir5} hairpin in a monocistronic mRNA, DROSHA-mediated excision of the hairpin leads to cleavage and subsequent degradation of the mRNA. Efficient cleavage of the mRNA should therefore be associated with reduced Venus expression. We examined the mean fluorescence intensity (MFI) of Venus in WT and Drosha KO 293T cells after transduction with the two vectors. Similar to the viral titer ratio in Figure 5A, we observed an ~40%

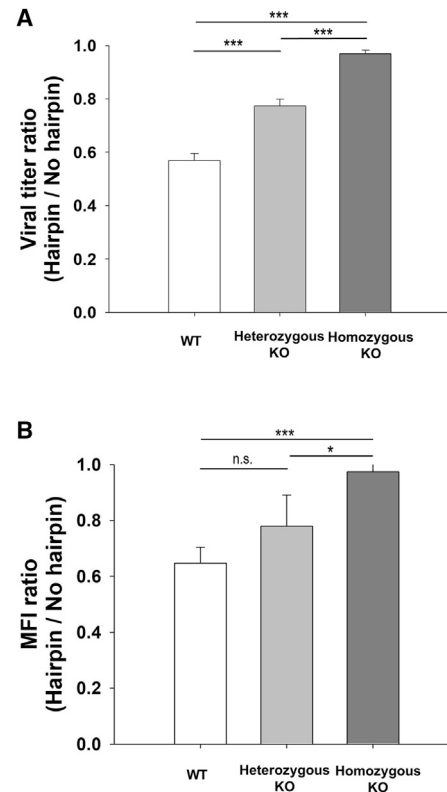


Figure 5. Viral Titers and Mean Fluorescence Intensity of Homozygous KO Cell Lines

(A) Ratios of viral titers of hairpin:non-hairpin-containing vectors produced in WT or homozygous Drosha KO cell lines. Titers were determined by serial dilutions of supernatants on MEL cells followed by FACS analysis for Venus expression. (B) Ratio of Venus mean fluorescence intensity (MFI) in homozygous KO:WT 293T cells lines infected with non-hairpin-containing (LeGO-SFFV) or hairpin shRNA^{mir5}-containing (LeGO-SFFV-shRNA^{mir5}) virus. MFI was calculated based on fluorescence intensity of Venus* 293T cells from FACS analysis. Error bars: SD (N = 4). *p < 0.05; ***p < 0.0005. n.s., not significant.

decrease in the expression as quantified by the MFI ratio of hairpin- to non-hairpin-transduced cells (Figure 5B). In contrast, in homozygous KO cells, we observed no decrease in the MFI ratio of integrated vectors. Cells with one functional DROSHA allele showed an intermediate phenotype with an MFI ratio between 0.7 and 0.8.

Rescued DROSHA Activity Is Associated with Restoration of Viral Titers in Packaging Cell Lines

Next, we performed a rescue experiment using a WT cDNA and a transdominant (TN) mutant of DROSHA. The latter contains two point mutations at E1045Q and E1222Q, which causes loss of catalytic activity of DROSHA (Figure 6A).²⁷ We tested the effect of re-expression of DROSHA in homozygous KO cells on the resulting titers on MEL cells. First, we confirmed the expression of DROSHA by immunoblot analysis. As seen in Figure 6B, both the WT DROSHA and the TN mutant protein are expressed in homozygous

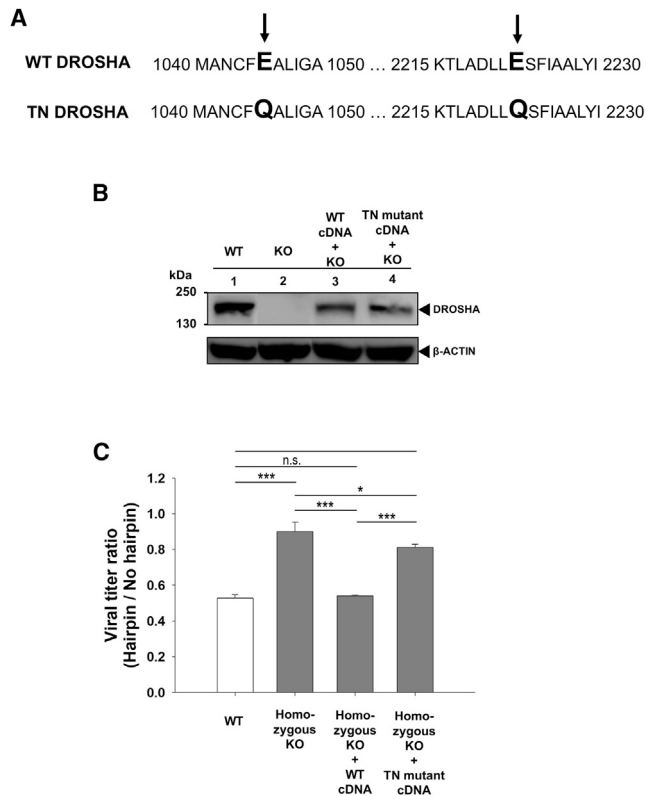


Figure 6. Re-expression of DROSHA in Homozygous KO Cells Leads to Reduced Viral Titer

(A) Protein sequence comparison of WT and TN mutant DROSHA. The mutant DROSHA has two point mutations at E1045Q and E1222Q, which causes loss in the catalytic activity of DROSHA. (B) Immunoblot analysis for recombinant DROSHA expression in homozygous KO cells. The position of DROSHA protein band is noted by arrowhead. β -ACTIN is used as a control shown at the bottom. (C) Ratio of viral titers of hairpin:non-hairpin vectors obtained after transfection of homozygous KO cell line co-transfected with WT *DROSHA* or TN *DROSHA* plasmid. Error bars: SD (N = 4). * $p < 0.05$; *** $p < 0.0005$. n.s., not significant.

KO cells. We transduced MEL cells using the virus generated from each producer population. The viral titer ratio decreased in the homozygous KO cells expressing WT DROSHA (Figure 6C) to levels similar to WT cells. Homozygous KO cells expressing TN DROSHA showed a modest reduction in viral titer compared with homozygous KO cells. The titer of TN DROSHA-expressing KO cells was significantly higher than either WT cells or KO cells expressing the WT DROSHA cDNA.

DISCUSSION

Viral vector-based RNAi gene therapy is a powerful approach to modulate clinically important genes. In this study, we show that reduction in viral titers generated in packaging cell lines of shRNA^{miR}-containing vectors is directly related to the cleavage of the full-length viral genomic transcripts by DROSHA. We used CRISPR technology to generate *DROSHA* KO in 293T packaging cells. In the absence of DROSHA, shRNA^{miR} hairpin-containing viral genomic

RNAs were not cleaved. This lack of viral genomic RNA processing in packaging cells was associated with restoration of viral titer comparable with non-hairpin-containing vector constructs. Additionally, there was no difference between the expression of the hairpin vector versus non-hairpin-containing vector in infected *DROSHA* KO cells, suggesting that *DROSHA* also does not cleave shRNA^{miR} hairpin-containing mRNA transcribed from the internal promoter of the integrated provirus. Finally, re-expression of WT DROSHA in homozygous KO cells led to a reduction in titer of hairpin-containing vectors. The difference in titer reduction in cells expressing the inactive mutant TN DROSHA versus WT DROSHA cDNAs strongly suggests that catalytic activity of DROSHA is important for the cleavage of shRNA^{miR} hairpin-containing viral genomic RNA.

These studies extend published work suggesting an important role for the microprocessor complex in disrupting packaging of shRNA-containing viral vectors. Previously, it was reported that the presence of shRNA^{miR} hairpin cassettes can negatively affect lentiviral vector titers, and inhibition of the RNAi pathway via saturation could rescue vector production.²⁴ In these studies, replacement of the cytomegalovirus promoter with an inducible promoter also resulted in restoration of the vector titer. In addition, it has been reported that inhibition of RNase III enzyme activity of DROSHA can increase titers of miRNA-encoding retroviruses.²⁸ Inhibition of DROSHA in the packaging cells resulted in impaired processing of mature miRNA from full-length retroviral transcripts, which led to more packaging of full-length viral transcripts into infectious virus particles. However, previous studies showed no direct proof of the cleavage of viral transcripts as a result of DROSHA activity and in association with the reduction in viral titers. Here, we report the generation of a packaging cell line that obviates that need for these manipulations and is the basis for an effective virus vector production system for all hairpin-containing constructs (Figure 7).

In summary, our data demonstrate the requirement of homozygous KO in producer cells for the efficient production of shRNA^{miR} hairpin viruses. Our findings have important implications for future production of viral shRNA^{miR}-containing vectors for RNAi-based therapy.

MATERIALS AND METHODS

Cloning of *DROSHA* Targeting CRISPR/Cas9 Plasmid

DROSHA targeting sgRNAs were designed using online CRISPR design tools developed by Feng Zhang and colleagues (<http://crispr.mit.edu/>)²⁶ and CHOPCHOP (<http://chopchop.cbu.uib.no/>).^{29,30} Two gRNAs targeting the 5' end of exon 4 (labeled gRNAs 1–2) of *DROSHA* and two gRNAs targeting the 3' end of exon 30 (labeled gRNAs 3–4) were subsequently utilized (Table S1). The guide strand oligo sequences were synthesized from Invitrogen Custom DNA Oligos (Thermo Fisher Scientific, Waltham, MA, USA), annealed, and inserted into BbsI sites of *S. pyogenes* Cas9 cloning vector with 2A-EGFP (pX458; Addgene plasmid ID: 48139) (Figure 6A). The GenBank file for the plasmid is available through Addgene.

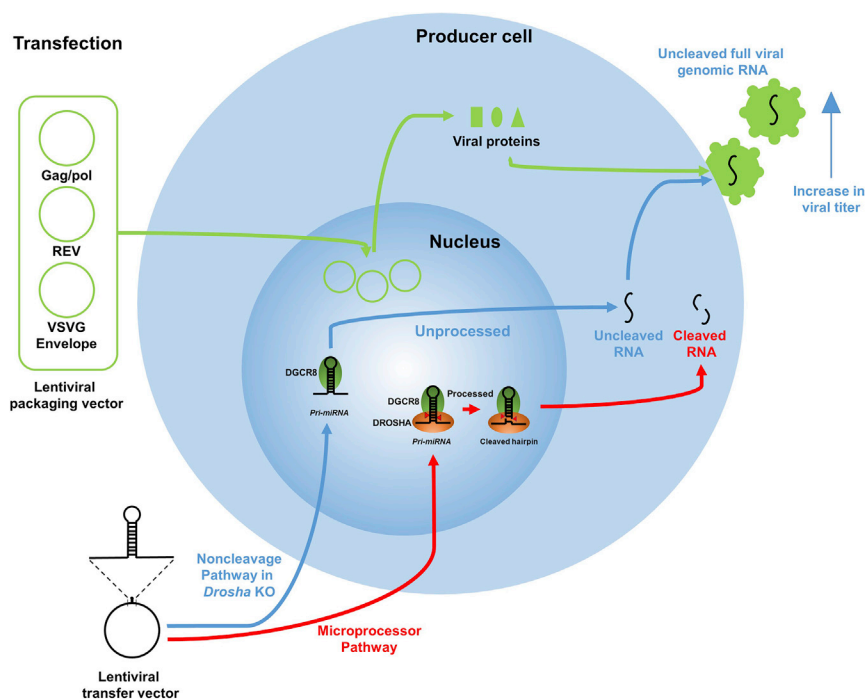


Figure 7. Schematic Representation of Non-cleavage Pathway of shRNA^{miR} by Homozygous KO Allowing Recovery of Full Viral Genomic RNA Titer

Packaging expression cassettes (Gag/Pol and REV), envelope expression cassette (VSV-G), and vector expression cassettes (shRNA^{miR}-containing lentiviral transfer vector) are used to generate lentiviral particles.

with a monoclonal anti-DROSHA rabbit antibody (Abcam, Cambridge, MA, USA) or mouse anti- β -actin (Sigma-Aldrich, St. Louis, MO, USA). Anti-rabbit and anti-mouse IgG HRP-linked secondary antibody (Cell Signaling, Danvers, MA, USA) was used for detection by chemiluminescence by SuperSignal West Dura Extended Duration Substrate (Thermo Scientific, Rockford, IL, USA).

Proliferation of *DROSHA* KO Cell Lines

For initial seeding of cells, the cell number was calculated using a hemocytometer and trypan blue dye to distinguish viable from dead cells.

Proliferation of cells was assessed using the fluorescence-based CyQUANT Cell Proliferation Assay (Invitrogen, Carlsbad, CA, USA) according to the manufacturer's instructions. 1,000 cells/well were plated in a 96-well plate, and fluorescence measurements were made using a microplate reader with excitation at 485 nm and emission detection at 530 nm.

Cell Culture

HEK293T/17 (ATCC CRL-11268) and MEL cells were maintained in DMEM or RPMI medium (Cellgro, Washington, DC, USA) supplemented with 10% fetal calf serum and 2% penicillin-streptomycin, respectively.

Generation of *DROSHA* KO Cell Lines

HEK293T/17 (ATCC CRL-11268) cells were transfected with CRISPR/Cas9 plasmids targeting *DROSHA*. We co-transfected 5' and 3' targeting gRNAs with 1 mg/mL linear polyethylenimine (PEI) (Polysciences, Warrington, PA, USA) and fluorescence-activated cell sorting (FACS) sorted for cells expressing high levels of GFP. Sorted cells were plated at low density, and individual clones were picked and expanded. The clones were screened by PCR analysis to identify *DROSHA* KO cell lines using a set of *DROSHA* primers (Table S2) and additionally analyzed for *DROSHA* expression by immunoblot analysis.

Immunoblot Analysis

DROSHA KO cell lines were lysed in radioimmunoprecipitation assay (RIPA) lysis buffer (Thermo Scientific, Rockford, IL, USA), with protease inhibitor (Roche, Mannheim, Germany). Samples were mixed suspended in 2 \times Laemmli sample buffer supplemented with beta-mercaptoethanol. The mixtures were denatured by boiling and loaded onto a 10% SDS-polyacrylamide gel. Electrophoresis was performed to separate each sample according to size and subsequently transferred to a polyvinylidene fluoride membrane (Millipore, Billerica, MA, USA). Following blocking in PBS with 0.1% Tween 20 and 5% nonfat dry milk, the polyvinylidene fluoride membrane was incubated

Construction of SFFV-BCL11A shRNA^{miR} Plasmids

A control non-hairpin-containing (LeGO-SFFV) lentiviral vector plasmid was constructed by removing the BCL11A shRNA^{miR} hairpin from the LeGO-SFFV-shRNA^{miR5} plasmid¹⁴ (Figure 2A). In LeGO-SFFV-shRNA^{miR5}, the shRNA is embedded in an hsa-miRNA223 (shRNA^{miR}) backbone to allow expression from pol II promoters in mammalian cells.

Lentivirus Production, Titration, and Transduction

Lentiviral vector supernatants were generated by co-transfecting 1 μ g of lentiviral transfer vector, 0.5 μ g of Gag/Pol, 0.25 μ g of REV, and 0.25 μ g of vesicular stomatitis virus (VSV-G) packaging plasmids into HEK293T cells in a 12-well plate using linear PEI reagent. Supernatants were collected at 48 hr after transfection and filtered through a 0.45- μ m polyvinylidene fluoride (PVDF) syringe filter (Corning Life Sciences, Tewksbury, MA, USA). To determine the titer, we infected 1×10^5 MEL cells in a 24-well plate with serial dilutions of the lentiviral vector supernatants in the presence of polybrene (8 μ g/mL) (Sigma-Aldrich, St. Louis, MO, USA) and analyzed them 3 days post-transduction by flow cytometry analysis using the BD FACS Fortessa (BD Biosciences, San Jose, CA, USA). Transductions of 293T *DROSHA* KO cell lines were performed on 2×10^4 cells/well

in a 24-well plate followed by flow cytometric analysis of Venus expression 3 days post-transduction.

RNA Extraction, Lentiviral Pellet, and Northern Blot Analysis

For northern blot analysis, total RNA was extracted from *DROSHA* KO cell lines 48 hr after transfection with lentiviral packaging plasmids. For the detection of viral genomic RNA in viral particles, virus supernatants were treated with Benzonase (Sigma-Aldrich, Saint Louis, MO, USA) to remove free RNA and DNA, followed by centrifugation at $13,000 \times g$ at 4°C overnight. Total RNA was extracted from viral pellets by concentrating the Benzonase-treated virus supernatant in a Beckmann XL-90 centrifuge using SW-28 swinging buckets. The total RNA was isolated using TRIzol reagent (Ambion, Austin, TX, USA), then resolved on a 15% polyacrylamide Tris-borate-EDTA (TBE) urea gel or formaldehyde/agarose gel for separation of small RNAs or viral genomic RNA, respectively. RNA was transferred to Hybond-N+ nylon membrane (Amersham, Piscataway, NJ, USA) and UV-crosslinked. The blots were prehybridized using PerfectHyb Plus Hybridization buffer (Sigma, St. Louis, MO, USA) at 42°C for 1 hr. The blot was probe-labeled with either γ -³²P-labeled ATP (Perkin Elmer) and hybridized at 42°C overnight, or with α -³²P-labeled dCTP (Perkin Elmer) at 58°C overnight. Blots were washed in 2× sodium citrate, 0.1% SDS at room temperature, and exposed to film. Forward and reverse sequences for REV-responsive element (RRE) probe were as follows: 5'-GCTTTGTTTCCTTGGGTTCTTG-3' and 5'-CCAGGAGCTGTTGATCCTTTAG-3'.

Statistical Analysis

All values are presented as the mean ± SD. Statistical significance was assessed by Student's t test. $p < 0.05$ was considered statistically significant.

SUPPLEMENTAL INFORMATION

Supplemental Information includes two tables and can be found with this article online at <https://doi.org/10.1016/j.omtn.2018.07.002>.

AUTHOR CONTRIBUTIONS

H.H.P., R.T., M.B., S.G., P.D., H.X., and C.B. conducted experiments. D.A.W., C.B., and R.I.G. designed experiments. H.H.P., R.T., C.B., R.I.G., and D.A.W. wrote the paper.

ACKNOWLEDGMENTS

We thank Chad Harris and Meaghan McGuinness for technical assistance, and Ronald Mathieu and Mahnaz Paktinat of the Pediatric Hematology/Oncology FACS facility for help with cell sorting and analysis. We thank Joshua Mendell (UTSW) for providing the Drosha WT and TN mutant expression vectors. We also thank Axel Schambach, Amanda McCabe, and Hiroto Horiguchi for discussion. This work was supported by NIH grants U01HL117720 (to D.A.W., R.G., and C.B.) and R01HL137848 (to D.A.W.).

REFERENCES

- Bartel, D.P. (2009). MicroRNAs: target recognition and regulatory functions. *Cell* 136, 215–233.
- Bartel, D.P. (2004). MicroRNAs: genomics, biogenesis, mechanism, and function. *Cell* 116, 281–297.
- Filipowicz, W. (2005). RNAi: the nuts and bolts of the RISC machine. *Cell* 122, 17–20.
- Haasnoot, J., and Berkhout, B. (2006). RNA interference: its use as antiviral therapy. *Handb. Exp. Pharmacol.* 173, 117–150.
- Kim, D.H., and Rossi, J.J. (2007). Strategies for silencing human disease using RNA interference. *Nat. Rev. Genet.* 8, 173–184.
- Stolas, D., Lerner, C., Burchard, J., Ge, W., Linsley, P.S., Paddison, P.J., Hannon, G.J., and Cleary, M.A. (2005). Synthetic shRNAs as potent RNAi triggers. *Nat. Biotechnol.* 23, 227–231.
- Grimm, D., Streetz, K.L., Jopling, C.L., Storm, T.A., Pandey, K., Davis, C.R., Marion, P., Salazar, F., and Kay, M.A. (2006). Fatality in mice due to oversaturation of cellular microRNA/short hairpin RNA pathways. *Nature* 441, 537–541.
- Giering, J.C., Grimm, D., Storm, T.A., and Kay, M.A. (2008). Expression of shRNA from a tissue-specific pol II promoter is an effective and safe RNAi therapeutic. *Mol. Ther.* 16, 1630–1636.
- McBride, J.L., Boudreau, R.L., Harper, S.Q., Staber, P.D., Monteys, A.M., Martins, I., Gilmore, B.L., Burstein, H., Peluso, R.W., Polisky, B., et al. (2008). Artificial miRNAs mitigate shRNA-mediated toxicity in the brain: implications for the therapeutic development of RNAi. *Proc. Natl. Acad. Sci. USA* 105, 5868–5873.
- Boudreau, R.L., Martins, I., and Davidson, B.L. (2009). Artificial microRNAs as siRNA shuttles: improved safety as compared to shRNAs in vitro and in vivo. *Mol. Ther.* 17, 169–175.
- Khan, A.A., Betel, D., Miller, M.L., Sander, C., Leslie, C.S., and Marks, D.S. (2009). Transfection of small RNAs globally perturbs gene regulation by endogenous microRNAs. *Nat. Biotechnol.* 27, 549–555.
- Grimm, D., Wang, L., Lee, J.S., Schürmann, N., Gu, S., Börner, K., Storm, T.A., and Kay, M.A. (2010). Argonaute proteins are key determinants of RNAi efficacy, toxicity, and persistence in the adult mouse liver. *J. Clin. Invest.* 120, 3106–3119.
- Martin, J.N., Wolken, N., Brown, T., Dauer, W.T., Ehrlich, M.E., and Gonzalez-Alegre, P. (2011). Lethal toxicity caused by expression of shRNA in the mouse striatum: implications for therapeutic design. *Gene Ther.* 18, 666–673.
- Guda, S., Brendel, C., Renella, R., Du, P., Bauer, D.E., Canver, M.C., Grenier, J.K., Grimson, A.W., Kamran, S.C., Thornton, J., et al. (2015). miRNA-embedded shRNAs for lineage-specific BCL11A knockdown and hemoglobin F induction. *Mol. Ther.* 23, 1465–1474.
- Brendel, C., Guda, S., Renella, R., Bauer, D.E., Canver, M.C., Kim, Y.J., Heeney, M.M., Klatt, D., Fogel, J., Milsom, M.D., et al. (2016). Lineage-specific BCL11A knockdown circumvents toxicities and reverses sickle phenotype. *J. Clin. Invest.* 126, 3868–3878.
- Sankaran, V.G., Menne, T.F., Xu, J., Akie, T.E., Lettre, G., Van Handel, B., Mikkola, H.K., Hirschhorn, J.N., Cantor, A.B., and Orkin, S.H. (2008). Human fetal hemoglobin expression is regulated by the developmental stage-specific repressor BCL11A. *Science* 322, 1839–1842.
- Bauer, D.E., and Orkin, S.H. (2015). Hemoglobin switching's surprise: the versatile transcription factor BCL11A is a master repressor of fetal hemoglobin. *Curr. Opin. Genet. Dev.* 33, 62–70.
- Xu, J., Peng, C., Sankaran, V.G., Shao, Z., Esrick, E.B., Chong, B.G., Ippolito, G.C., Fujiwara, Y., Ebert, B.L., Tucker, P.W., and Orkin, S.H. (2011). Correction of sickle cell disease in adult mice by interference with fetal hemoglobin silencing. *Science* 334, 993–996.
- Gregory, R.I., Yan, K.P., Amuthan, G., Chendrimada, T., Doratotaj, B., Cooch, N., and Shiekhattar, R. (2004). The Microprocessor complex mediates the genesis of microRNAs. *Nature* 432, 235–240.
- Han, J., Lee, Y., Yeom, K.H., Kim, Y.K., Jin, H., and Kim, V.N. (2004). The Drosha-DGCR8 complex in primary microRNA processing. *Genes Dev.* 18, 3016–3027.
- Han, J., Lee, Y., Yeom, K.H., Nam, J.W., Heo, I., Rhee, J.K., Sohn, S.Y., Cho, Y., Zhang, B.T., and Kim, V.N. (2006). Molecular basis for the recognition of primary microRNAs by the Drosha-DGCR8 complex. *Cell* 125, 887–901.
- Partin, A.C., Ngo, T.D., Herrell, E., Jeong, B.C., Hon, G., and Nam, Y. (2017). Heme enables proper positioning of Drosha and DGCR8 on primary microRNAs. *Nat. Commun.* 8, 1737.

23. Kwon, S.C., Nguyen, T.A., Choi, Y.G., Jo, M.H., Hohng, S., Kim, V.N., and Woo, J.S. (2016). Structure of Human DROSHA. *Cell* *164*, 81–90.
24. Liu, Y.P., Vink, M.A., Westerink, J.T., Ramirez de Arellano, E., Konstantinova, P., Ter Brake, O., and Berkhout, B. (2010). Titers of lentiviral vectors encoding shRNAs and miRNAs are reduced by different mechanisms that require distinct repair strategies. *RNA* *16*, 1328–1339.
25. Ha, M., and Kim, V.N. (2014). Regulation of microRNA biogenesis. *Nat. Rev. Mol. Cell Biol.* *15*, 509–524.
26. Ran, F.A., Hsu, P.D., Wright, J., Agarwala, V., Scott, D.A., and Zhang, F. (2013). Genome engineering using the CRISPR-Cas9 system. *Nat. Protoc.* *8*, 2281–2308.
27. Rakheja, D., Chen, K.S., Liu, Y., Shukla, A.A., Schmid, V., Chang, T.C., Khokhar, S., Wickiser, J.E., Karandikar, N.J., Malter, J.S., et al. (2014). Somatic mutations in DROSHA and DICER1 impair microRNA biogenesis through distinct mechanisms in Wilms tumours. *Nat. Commun.* *2*, 4802.
28. Brandl, A., Wittmann, J., and Jäck, H.M. (2011). A facile method to increase titers of miRNA-encoding retroviruses by inhibition of the RNaseIII enzyme Drosha. *Eur. J. Immunol.* *41*, 549–551.
29. Montague, T.G., Cruz, J.M., Gagnon, J.A., Church, G.M., and Valen, E. (2014). CHOPCHOP: a CRISPR/Cas9 and TALEN web tool for genome editing. *Nucleic Acids Res.* *42*, W401–W407.
30. Labun, K., Montague, T.G., Gagnon, J.A., Thyme, S.B., and Valen, E. (2016). CHOPCHOP v2: a web tool for the next generation of CRISPR genome engineering. *Nucleic Acids Res.* *44* (W1), W272–W276.